The imaginary component of permittivity is related to $Q_F$ by

$$K_F' = \frac{K_F}{Q_F} = K_F \tan \delta' \qquad (9)$$

where $\tan \delta'$ is the dissipation factor.

In order to test the technique, a Mylar sheet 1 mil thick was measured at 2.8 GHz. A $K_F$ of 2.21 and $\tan \delta'$ of 0.0035 were found experimentally; these values show excellent agreement with the corresponding published values [3] of 2.20 and 0.003, respectively.

The technique described above was used to measure the properties of a silicon monoxide (SiO) film at $S$-band. The cavity for these measurements is shown in Fig. 3. It is convenient to measure the real part of the permittivity with the dielectric film deposited on the end plate A of the cavity and the imaginary part with the film deposited on the post B.

Plate A should be baked at a temperature exceeding the maximum temperature encountered during formation of the film. The cavity with the baked but uncoated end plate is calibrated by obtaining a curve of resonant frequency as a function of gap space. The gap space is controlled by placing washers of known thickness under surface C and a weight on surface D. Airholes E are used to permit smooth and repeatable motion of the center post. There is an initial gap (with no washers present) to prevent damage to the films. The calibration curve is found with the various washers inserted. Each point on the curve is the average of ten frequency readings. The spread at each point is less than 2.3 MHz.

After the calibration is completed, plate A is removed and coated. The film geometry and location are controlled by either mechanical masking or photoresist techniques. Plate A is replaced and a new curve of frequency as a function of gap spacing is determined, once again averaging over a large number of frequency readings for each washer.

It is desirable to use a high unloaded $Q$ cavity for measurement of the imaginary component of permittivity. This cannot be achieved with a removable lower plate since the high-current path at the plate edges will be interrupted by the space between the plate and the cavity body. Therefore, for the $Q$ measurement, a cavity similar to that discussed above is used. The end plate of this cavity is brazed into place and the film is deposited on the end of the center post. While it is inconvenient to use two cavities, better accuracy can be obtained for each of the measurements. The two cavities used in the tests reported below showed nearly identical performance.

Some typical calibration and perturbation curves for an SiO film are shown in Fig. 4. The resonant frequency is plotted as a function of washer thickness.

A 10$\mu$ thick film was vacuum-deposited through a mechanical mask at a rate of 2500 Å/min from a source at 1250°C onto an aluminum substrate at an average temperature of 95°C. Figure 5 shows a plot of $K_F$ as a function of $d_2$. The departure from a linear $d_1$-$d_2$ relationship is reflected in the large change in $K_F$. This occurs when a spacing is reached where the capacitance calculation is no longer valid. The dielectric constant of the SiO film used in Fig. 5 is found to be 4.2

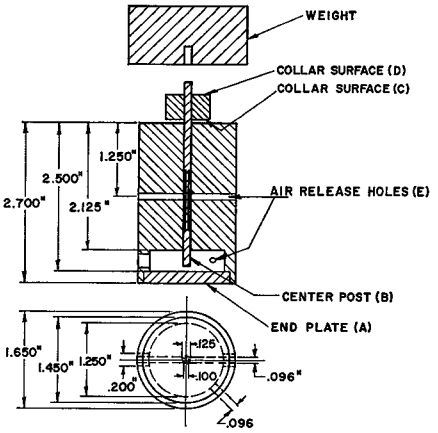


Fig. 3. Cavity used in tests.

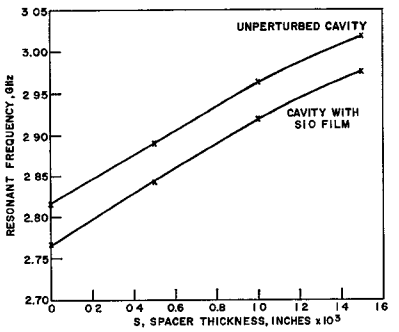


Fig. 4. Resonant frequency as a function of washer thickness for perturbed and unperturbed cavities.

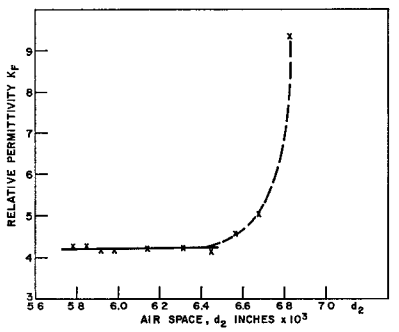


Fig. 5. $K_F$ of SiO as a function of $d_2$, at $S$-band.

at $S$-band. Tests on other films showed values between 4 and 5. The low-frequency dielectric constant at 1 MHz of these films was between 5 and 5.5. This is consistent with published [4] values at 1 MHz.

The $Q_F$ of the SiO film at $S$-band (2894 MHz) was found to be 34.3 corresponding to $\tan \delta' = 0.0292$. The $\tan \delta'$ of the film at 1 MHz was 0.018 compared with the published value of 0.015.

The accuracy obtainable with the method described above is determined by the ability to control in known steps the gap spacing; such accuracy also requires a precise value of film thickness. The calculation of $K_F$ involves taking a difference between two similar numbers, and can result in large errors unless the spacings are precisely known. Equation (5) shows that to keep a constant accuracy, thicker films are required for higher dielectric constants.

As an example of the degree of accuracy that careful work can result in, the thickness of a 1$\mu$ film with a dielectric constant of nearly 20 was measured by the cavity technique with an accuracy of better than ten percent. In general, however, it is suggested that films of at least 10$\mu$ thickness be used.

In summary, a perturbation method for measuring the complex permittivity of dielectric films at microwave frequencies has been demonstrated. Results can be obtained from straightforward measurements and calculations.

### Acknowledgment

The authors are pleased to thank W. Kritzler for his assistance during the early development of the method. The help of R. Chamberlain in providing the films tested is gratefully acknowledged.

H. Sobol
J. J. Hughes
RCA Laboratories
Princeton, N. J.

### References

[1] A. R. Von Hippel, *Dielectric Materials and Applications*. New York: Wiley, 1954.
[2] B. Lax and K. J. Button, *Microwave Ferrites and Ferrimagnetics*. New York: McGraw-Hill, 1962.
[3] A. R. Von Hippel, *loc. cit.*, p. 178.
[4] F. S. Maddocks and R. E. Thun, "Properties of evaporated film capacitors," *J. Electromech. Soc.*, vol. 109, pp. 99–103, February 1962.

## Experimental 4-Port E-Plane Junction Circulators

### Introduction

This correspondence reports on the experimental investigation of broadbanding 4-port $E$-plane cross-junction circulators. The circulator experiments were carried out in $X$-band (WG 16). From previous work on 3-port $E$-plane circulators[1] it was decided to adopt a ferrite configuration using two flat disks positioned against the narrow walls at the intersection of the crossed waveguides as shown in Fig. 1. The ferrite disks are magnetized by a dc magnetic field parallel to the ferrite axis.

The investigation was empirical as a theoretical treatment is complicated by the variation of RF magnetic field in the direction of the dc polarizing field. There were three stages in the development of this device: the search for a circulating mode which allows broadbanding techniques to be applied, adjustments of the operating frequency, and high-power tests on the optimized configuration.

Manuscript received October 31, 1966; revised January 30, 1967. This paper was presented at the International Conference on Microwave Behavior of Ferrimagnetics and Plasmas, London, England, September, 1965.

[1] L. E. Davis and S. R. Longley, "$E$-plane 3-port $X$-band waveguide circulators," *IEEE Trans. on Microwave Theory and Techniques (Correspondence)*, vol. MTT-11, pp. 443–445, September 1963.

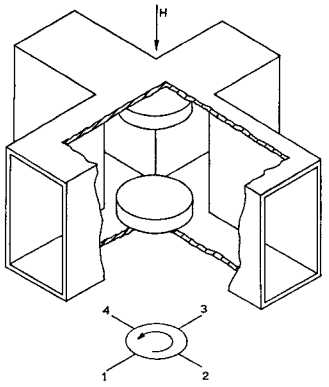


Fig. 1. 4-port $E$-plane junction circulator.

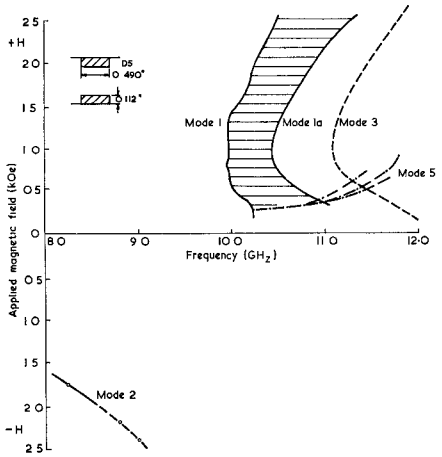


Fig. 2. Mode chart for the $E$-plane circulator.

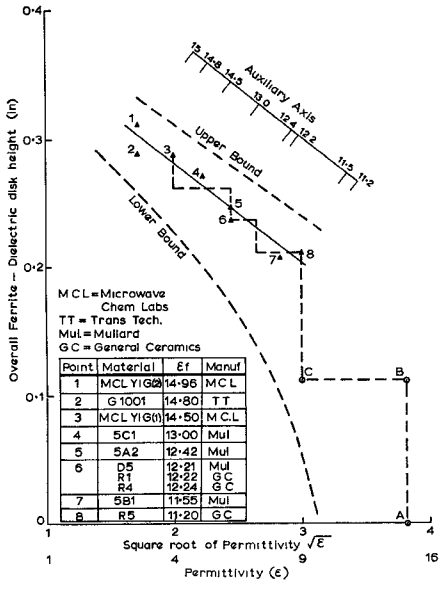


Fig. 3. Design nomogram used to optimize the bandwidth.

## Experimental Procedure

To investigate the modes of circulation the microwave frequency was increased in discrete steps, and at each frequency the outputs from ports 2 and 4 were monitored as the applied field was swept from 0 to 2500 Oe. Only those modes were recorded where the difference in insertion loss between ports 1 and 2 and between ports 1 and 4 was greater than 10 dB. This information is represented in Fig. 2 by plotting the applied magnetic field $H$ against frequency, with circulation in the reverse direction represented by a negative applied field.

The modes are arbitrarily numbered; the distinction in direction has been made by giving all modes in one direction odd numbers and in the other, even. The best performance is obtained with modes 1 and 1a. The shaded region between these modes indicates a broadband isolation region with peaks in the isolation characteristic corresponding to mode 1 and mode 1a. Only narrow bandwidths are observed using other modes. Figure 2 does not give an indication of the cross decoupling, that is, the degree of decoupling of port 3 from port 1. As it is necessary to optimize the isolation and cross decoupling characteristics at the same value of applied magnetic field, adjustment of the ferrite diameter is required. When this is done a narrowband circulator is first produced.

Broadbanding is achieved by using a stack of thin dielectric disks of diminishing dielectric constant on top of each piece of ferrite. The dielectric diameter was arbitrarily fixed and the dielectric disk height and permittivity were adjusted for maximum bandwidth corresponding to an isolation characteristic on ports 3 and 4 of better than 20 dB. This matching procedure was applied with ferrites of different heights, and it was found that the greatest bandwidth was achieved with ferrite between 0.112 inch and 0.122 inch high. This technique, using a manganese-magnesium ferrite (Mullard Ferroxcube D5), gave the following performance:

| | |
|---|---|
| Isolation | 1–4 >20 dB |
| Isolation | 1–3 >20 dB |
| Insertion loss | 1–2<0.8 dB |
| Bandwidth | 6 percent. |

Nine other polycrystalline ferrite and garnet materials were tested with saturation magnetizations in the range 1000–2200 gauss, and with linewidths between 55–450 Oe. The permittivity of these materials varied between 11 and 15 (Table I). The matching procedure was found to be independent of linewidth and magnetization but the choice of the permittivity and height of the dielectric disks was dependent on the dielectric constant of the ferrite.

TABLE I

Ferrite Parameters

| Ferrite | | $4\pi Ms$ | $\Delta H$ | Quoted $\epsilon f$ | Measured $\epsilon f$ | $g$ | tan $\delta$ |
|---|---|---|---|---|---|---|---|
| R1 | (Mg Mn) | 1760 | 490 | — | 12.22 | 2.11 | 0.0008 |
| R4 | (Mg Mn) | 1780 | 380 | — | 12.24 | 2.05 | 0.0008 |
| R5 | (Mg Mn Al) | 1110 | 220 | — | 11.20 | 2.03 | 0.0005 |
| MCL-YIG(1) | (YIG) | 1750 | 55 | — | 14.50 | 2.00 | 0.002 |
| G1001 | (YGdIG) | 1200 | 85 | 15 | 14.80 | 2.00 | 0.0005 |
| D5 | (Mn Mg) | 2150 | 450 | 12 | 12.21 | 2.10 | — |
| E6 (5C1) | (Mn Al) | 1850 | 150 | 14 | 13.0 | 2.02 | — |
| E5 (5B1) | (Mn Al) | 1045 | 175 | 11 | 11.55 | 2.05 | — |
| E3 (5A2) | (Mn Al) | 1450–60 | 245 | 13 | 12.42 | 2.05 | — |
| MCL-YIG(2) | (YIG) | 1750 | 55 | — | 14.96 | 2.00 | 0.002 |
| R6 | (Mn Mg Al) | 730 | 120 | — | 10.60 | 2.01 | — |

Figure 3 is a plot of overall height of each stack of ferrite and dielectric disks against square root of permittivity of the disks. Points 1–8 represent the overall height and the permittivity of the final disk for the ferrites indicated in Table I. It has been found experimentally that the disk permittivity should lie within the bounds of the limit curves shown for broadband operation.

Using Fig. 3 it is possible to match a ferrite of known permittivity, lying within the range covered, by choosing a number of dielectric disks which form a "staircase" as shown on the curve lying within the bounds indicated. The overall height of the combination and the dielectric constant of the final disk lie on the curve drawn through points 1–8.

## Experimental Results

The largest bandwidth obtained was 8 percent using YIG (2) [Fig. 4(a)]; final external screw matching was applied to the circulator in order to further improve the 1–3 isolation characteristic.

The insertion loss (<0.7 dB) is rather large for present-day applications owing to two factors:

1) The high-loss tangent of this particular ferrite (0.002).

2) The loss tangent of the matching dielectric disks.

Although it has not been possible to make a direct comparison[2] between two undoped garnet materials, using a doped YIG (G1001) with a loss tangent <0.005 and approximately the same disk matching structure, a bandwidth of 4½ percent for an insertion loss <0.5 dB is obtained [Fig. 4(b)].

Variation of the dielectric disk diameter has, in some instances, improved the bandwidth. In the case of D5, as shown in Fig. 4(c), there is a bandwidth in excess of 6 percent.

Another method of matching is to shape the dielectric in the form of a frustrum of a cone. Comparable bandwidths have been observed.

The ten ferrites used produced circulators working below 9.2 GHz. To shift the operating band to higher frequencies without scaling

[2] J. W. Simon, "Broadband strip-transmission line $Y$-junction circulators," presented at the Western Electronic Show and Convention (WESCON), San Francisco, Calif., August 20–23, 1963.

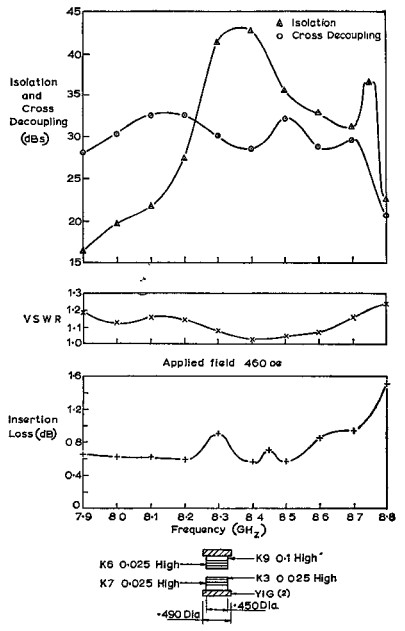


(a). Performance of YIG (2) with constant-diameter dielectric disks.

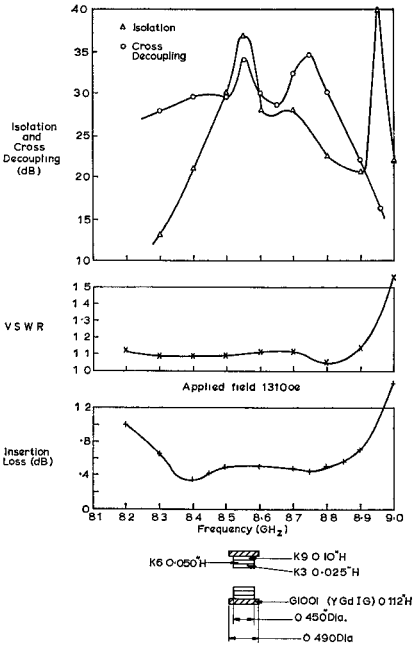


(b). Performance of YGdIG with constant-diameter dielectric disks, showing the decreased insertion loss compared with Fig. 4(a).

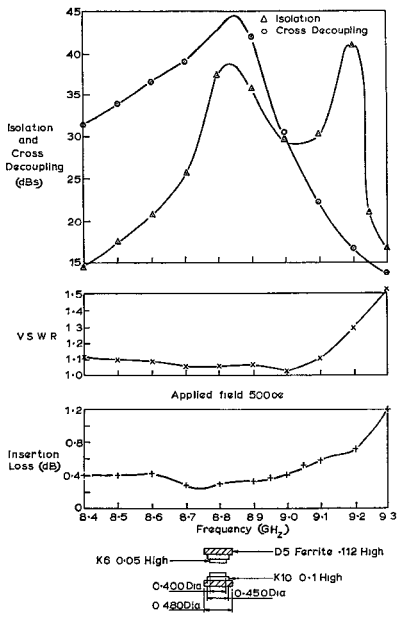


(c). An improved bandwidth is obtained for D5 ferrite by varying the dielectric geometric structure.

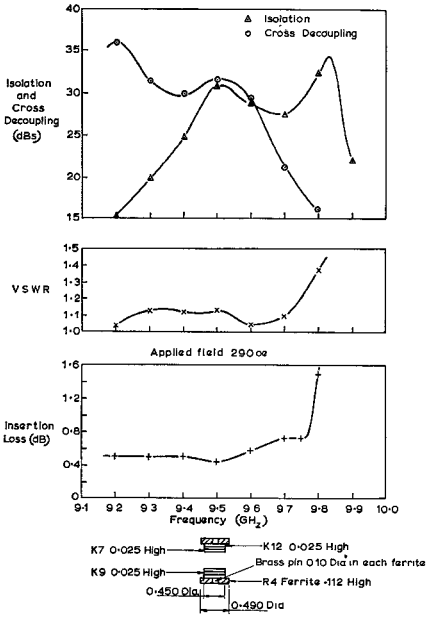


(d). Typical example of the change in frequency produced by the introduction of a conducting pin into the ferrite (R4).

Fig. 4.

the waveguide has proved difficult but two methods have been tried. The first was to use ferrite with a central conducting pin [Fig. 4(d)]. Here the operating bandwidth has been shifted up to 500 MHz with a conducting pin of 0.10-inch diameter. Larger-diameter pin sizes have resulted in increased insertion loss. The other method of increasing the frequency was to reduce the height of the junction by the introduction of conducting disks under the ferrite. The bandwidth shifted only slowly with relatively large conducting disks.

The $E$-plane circulator geometry is less liable to breakdown than an $H$-plane device; we have observed no breakdown up to power levels of at least 60 kW peak. The isolation characteristics are unchanged with all the materials examined at these power levels. There is, however, an increase in insertion loss with power level; the material with the lowest increase is manganese-aluminum ferrite (Ferroxcube 5B1), with a saturation magnetization of 1045 gauss. This circulator handled a mean power of 40 watts with a duty cycle of 0.001, and gave the following performance at 9.0 GHz:

| | |
|---|---|
| Isolation | 1–4 >20 dB |
| Isolation | 1–3 >20 dB |
| Insertion loss | 1–2 <0.7 dB |
| VSWR | 1.13. |

This circulator is compact and some improvement in insertion loss can be expected with better materials. Larger bandwidths appear possible with variation on the previously mentioned matching techniques.

S. R. Longley[3]
Mullard Research Labs.
Redhill, Surrey, England

[3] Mr. Longley is now engaged in postgraduate studies at University College, London.

## Gap Spacing for End-Coupled and Side-Coupled Strip-Line Filters

Two of the simplest strip-line configurations for bandpass filters are those which utilize end coupling [1], [2] (Fig. 1) and side coupling [3] (Fig. 2). For the special case of a symmetric strip line with center conductor of negligible thickness (Fig. 3), it is possible to establish expressions which explicitly relate gap spacing $S$ to normalized bandwidth $w$. Generally it is found that the greater the gap width, the less important are the tolerance considerations; alternatively, a broader bandwidth may be achieved for a given tolerance. The purpose of this correspondence is to establish a criterion that will enable a designer to select the filter with the greater coupling gap for given values of ground plane spacing $D$, midband wavelength $\lambda_0$, and normalized bandwidth.

The equivalent circuit of a series gap in an end-coupled filter (center-line representation) comprises a series capacitance $C_1$ and two shunt capacitances $C_2$ (Fig. 4). Approximate analytic relations are available [4] which relate the normalized susceptances associated with $C_1$ and $C_2$ to $S$, $D$, and $\lambda_0'$ $(=\lambda_0/\sqrt{\epsilon_r})$:

$$b_1 = \frac{D}{\lambda_0'} \ln \left\{ \coth \left( \frac{\pi}{2} \cdot \frac{S}{D} \right) \right\} \qquad (1)$$

$$b_2 = \frac{-2D}{\lambda_0'} \ln \left\{ \cosh \left( \frac{\pi}{2} \cdot \frac{S}{D} \right) \right\}. \qquad (2)$$

Equations (1) and (2) are valid for $W/D > 0.35$ and $T/D < 0.1$. Experimental evidence for their accuracy has been obtained by Oliner [5], where $b_1$ and $b_2$ are plotted as a function of $S/W$. As $S/D$ decreases, $b_1$ rapidly rises (theoretically to infinity) while $b_2$ slowly decreases (theoretically to zero). In particular, for $S/D < 0.2$, $b_1 > 10\,|b_2|$, and for $S/D < 0.1$, $b_1 > 100\,|b_2|$. Assuming that $S/D$ is sufficiently small, $b_2$ can be neglected and the analysis that follows is considerably simplified.

The normalized susceptance of the $(i+1)$th gap of an end-coupled filter with $n$ stages,

Manuscript received November 28, 1966.